Presented at the Institute of Navigation National Technical Meeting, San Diego CA, 24-27 January 2005

Performance Trials of an Integrated Loran/GPS/IMU Navigation System, Part I

Gregory Johnson, Ruslan Shalaev, *John J. McMullen Associates*
Peter Swaszek, *University of Rhode Island*
Richard Hartnett, *U.S. Coast Guard Academy*

BIOGRAPHY

Gregory W. Johnson is the Director of the New London Office, John J. McMullen Associates, responsible for contracts for the Coast Guard R&D Center in Groton, CT. One of the principal projects he is currently working on is providing research assistance to the Coast Guard Academy. Mr. Johnson holds a BSEE from the Coast Guard Academy (1987), a MSEE from Northeastern University (1993), and is currently working toward a Ph.D. at the University of Rhode Island.

Peter F. Swaszek is a Professor of Electrical and Computer Engineering at the University of Rhode Island. He received his Ph.D. in Electrical Engineering from Princeton University. His research interests are in digital signal processing with a focus on digital communications systems.

Richard J. Hartnett received the BSEE degree from the U. S. Coast Guard Academy (USCGA) in 1977, the MSEE degree from Purdue in 1980, and the Ph.D. EE from the University of Rhode Island in 1992. He holds the grade of Captain in the U. S. Coast Guard, and is Head of Electrical and Computer Engineering at the USCG Academy. CAPT Hartnett has been a faculty member at USCGA since 1985, and is serving as National Marine Representative, Institute of Navigation (ION) Council. He is the 2004 winner of the International Loran Association Medal of Merit.

ABSTRACT

The Federal Aviation Administration (FAA) is currently leading a team consisting of members from Industry, Government, and Academia to provide guidance to the policy makers in their evaluation of the future of Loran-C in the United States. In a recently completed Navigation Transition Study, the FAA concluded that Loran-C, as an independent radionavigation (RNAV) system, is theoretically the best backup for the Global Positioning System (GPS). However, in order for Loran-C to be considered a viable back-up system to GPS, it must be able to meet the requirements for non-precision approaches (NPA's) for the aviation community, and the Harbor Entrance and Approach (HEA) requirements for the maritime community. Through FAA sponsoring, the U.S. Coast Guard Academy (USCGA) is responsible for conducting some of the tests and evaluations to help determine whether Loran can provide the accuracy, availability, integrity, and continuity to meet these requirements. A major part of assessing the suitability of Loran is in understanding the nature of Loran ground wave propagation over paths of varying conductivities and terrain. Propagation time adjustments, called "additional secondary factors (ASFs)," are used to adjust receiver times of arrival (TOAs) to account for propagation over non-seawater path(s). These ASFs vary both spatially and temporally, and unless understood and/or modeled, we lose accuracy and may not be able to guarantee a hazardously misleading information (HMI) probability of less than 1x10-7.

The Coast Guard Academy has been conducting a series of tests on a new integrated Loran/GPS/IMU receiver in the Thames River. This receiver integrates IMU information (velocity and acceleration) and ASF data from a stored grid into the Loran position solution to improve the accuracy and consistency of the resulting position. The density of the ASF grid used is based upon our previous study (ION AM June 2004); points in between the grid values are calculated by the receiver using a linear interpolation. The GPS information (position, time) is used to measure the ASF values in real-time to track deviations from the stored ASF grid. These grid differences are used to correct the grid values in the absence of a local ASF monitor station. Performance of the receiver using different ASF grids and interpolation techniques and corrected using the real-time calculated grid differences is shown. Finally, how all of these efforts lead towards meeting the accuracy requirements is shown.

INTRODUCTION

Contrary to what some may believe, Loran-C is still alive and in use worldwide. The United States is served by the North American Loran-C system made up of 29 stations organized into 10 chains (see Figure 1). Loran coverage is available worldwide as seen in Figure 2.

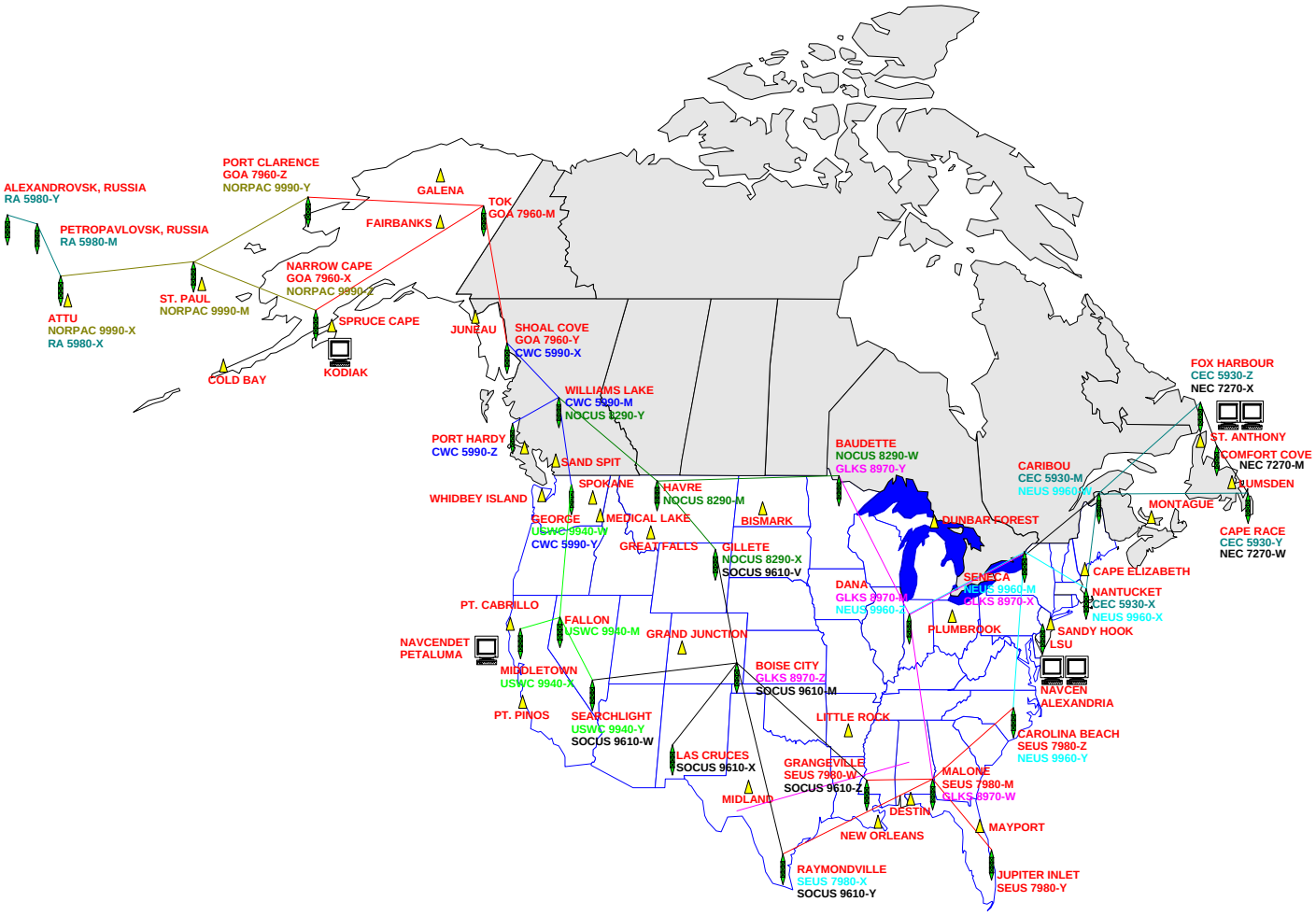

Figure 1 – North American Loran-C System

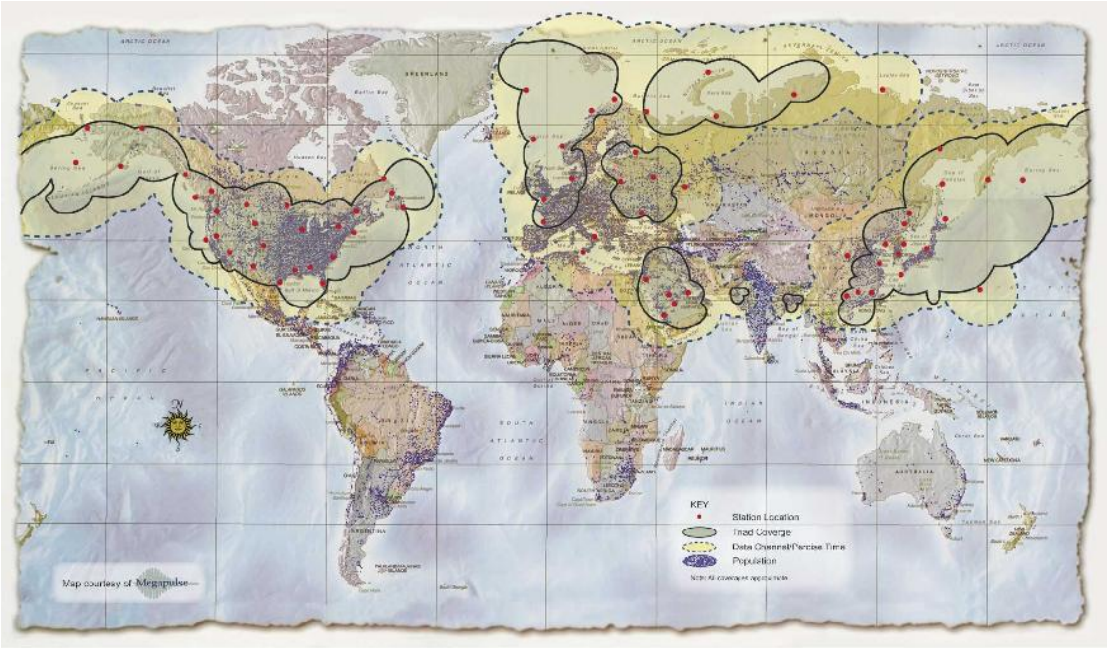

Figure 2 – Worldwide Loran Coverage

Given the ubiquity and quality of service available from the Global Positioning Service (GPS), one might wonder of what use is a system that has been operational since the 1970's? The answer is that Loran is an excellent backup system for GPS. As discussed in many sources, such as the Volpe vulnerability study [1], GPS is vulnerable to both intentional and unintentional jamming. Since Loran is a totally different system and subject to different failure modes than GPS, it can act as an independent backup system that functions when GPS does not. The Federal Aviation Administration (FAA) observed in its recently completed Navigation and Landing Transition Study [2] that Loran-C, as an independent radio navigation system, is theoretically the best backup for GPS; however, this study also observed that Loran-C's potential benefits hinge upon the level of position accuracy actually realized (as measured by the 2 drms error radius). For aviation applications this is the ability to support non-precision approach (NPA) at a Required Navigation Performance (RNP) of 0.3 which equates to a 2 drms error of 309 meters and for marine applications this is the ability to support Harbor Entrance and Approach (HEA) with 8-20 m of accuracy.

In this paper we will first provide a background and description of ASFs. We will then discuss the work on developing an accurate ASF grid and then the integrated receiver consisting of a Loran, GPS and IMU integrated using a Kalman filter.

ASF GRIDS

The biggest limitation on meeting the accuracy requirements is the spatial and temporal variations in Time of Arrival (TOA) observed by the receiver and presented to the position solution algorithm. This variation has been studied and presented in previous works [3-5]. The key to overcoming this limitation are Additional Secondary Factors (ASFs). A typical Loran receiver works on the simplifying assumption that the Loran signal propagates at a constant velocity – that of an electromagnetic wave in atmosphere over seawater. This is clearly not the case in most circumstances as the path from a given Loran station and a receiver may traverse a variety of terrain. The ASF accounts for the delay in the signal due to the propagation over non-seawater paths. This delay is due to terrain features; topography and obstacles along the path as well as the non-uniform (and lower) conductivity of land as opposed to seawater. The ASF value is used to adjust the receiver's estimate of the TOA of the Loran signal. It can be in the range of 1 to 8 microseconds across the continental U.S. (CONUS). What is more troubling to a receiver is that it can vary by as much as 1 to 2 microseconds in a local area such as a harbor or airport. A typical variation is shown in Figure 3.

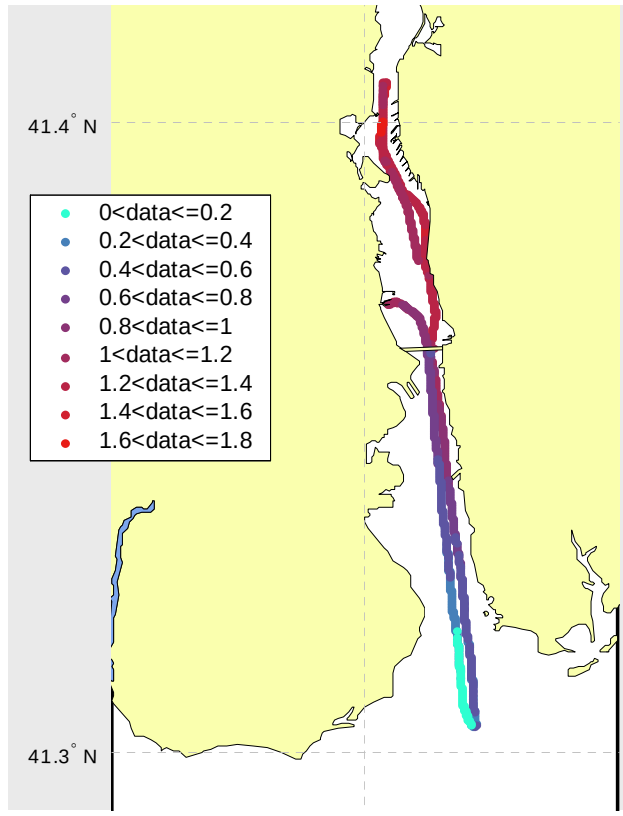

Figure 3 – Typical ASF variation in New London, CT. Here the 9960-X Station, Nantucket.

In order to account for this variation and increase the position accuracy, an ASF spatial correction must be used. There are two approaches for this. For the aviation community, with the easier accuracy target of 309m, the approach is to use a single set of ASF values (one for each Loran station) for each airport or airport approach depending upon the severity of the ASF gradients at that airport. For the maritime community with the more stringent accuracy requirement of 20m, a spatial grid of ASF values is used to capture more precisely the range of ASF values spatially. In addition, this grid needs to be adjusted for temporal variations. One method for this is to use a local reference station and broadcast corrections (differential Loran). These approaches have been discussed in the past [6-8].

One method of generating ASF spatial grids is through the use of a prediction tool such as BALOR [9, 10]. This software, developed by the University of Wales, Bangor, calculates the predicted ASFs for a point using the Monteath integral solution method using DTED level 1 terrain data, the FCC conductivity database, and coastline vectors. We have used this tool to generate predicted ASF grids for the Thames river area at a resolution of 0.0001 degrees. An example grid is shown in Figure 4. Unfortunately, if you compare Figure 4 to Figure 3, you

can see that the BALOR prediction tends to underestimate the full range of the ASF variation. This was discussed in more depth in [7, 8].

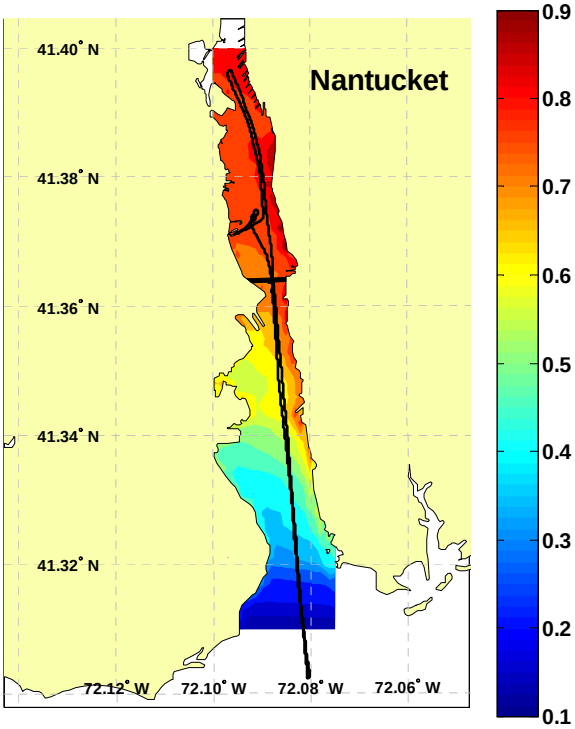

Figure 4 – BALOR ASF grid for the Thames River, CT for Nantucket.

The predicted grid was useful, however, for investigations into the use of a less dense grid of points. Using a sparser grid makes the distribution and storage of the ASF grids easier. This investigation [7] suggested that a coarse grid of 7x12 points (Figure 5) could be used and still retain sufficient accuracy. The receiver would interpolate between the grid points using bilinear interpolation.

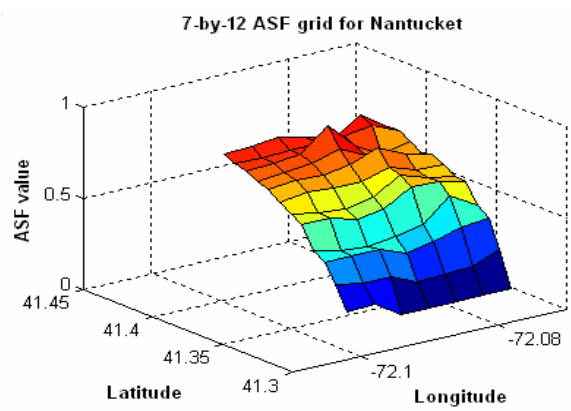

Figure 5 – BALOR data for 7x12 point coarse grid for Thames River.

In order to generate a grid of real ASF values, data was collected in the Thames River using one of the USCG Academy's T-boats (Figure 6). The data collection system and prototype integrated receiver is shown in Figures 7 and 8. The workings of the ASF collection system are described fully in [11]. In the Thames River, the four best Loran stations are Nantucket, Seneca, Carolina Beach, and Caribou (ordered by decreasing strength). Their relative positions are shown in Figure9.

Figure 6 – USCG Academy T-boat on Thames River.

Figure 7 – ASF measurement system, front showing laptop, HP counter, and LRSIIID Loran receiver.

Figure 8 – ASF measurement system, back showing IMU.

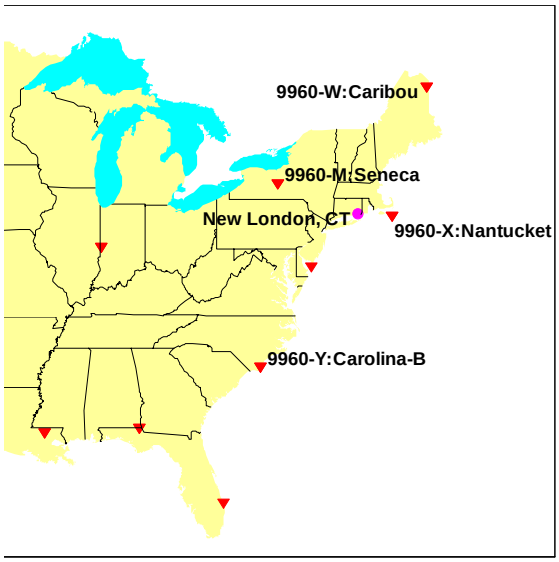

Figure 9 – Loran stations in receivable in New London, CT.

Using data from a number of trips on the river, a 7x12 ASF grid was constructed for each station. Figure 10 shows the paths the vessel took on the data collection trips. Each position where ASFs were measured (5 sec intervals) is color-coded in the figure to indicate which grid point (red dots) they are mapped to. Each measured ASF value was mapped to the closest grid point and then the median value of all measured values near each grid point was calculated. As an indicator of how good this median value is, standard deviations were calculated for each grouping of measured data. Some statistics on the standard deviations for the 84 grid points are shown for each of the 4 Loran stations in Table 1. As can be seen, some of the grid points are very good (standard deviations of measurements 2-3 ns), but some are very poor (standard deviations of as much as 2.8 microseconds!). The median values for all of the stations are on the order of 160-180ns, which is not great accuracy on the ASF measurements.

Table 1 – Standard Deviations of ASF Measurements on the 84 grid points for each of the 4 Loran stations (in microseconds)

	Seneca	Caribou	Nantucket	Car. Bch
Min	0.0028	0.0028	0.0021	0.0042
Max	2.7670	0.6772	0.9172	0.6353
Median	0.1624	0.1604	0.1232	0.1829
Mean	0.2379	0.2350	0.1477	0.2365

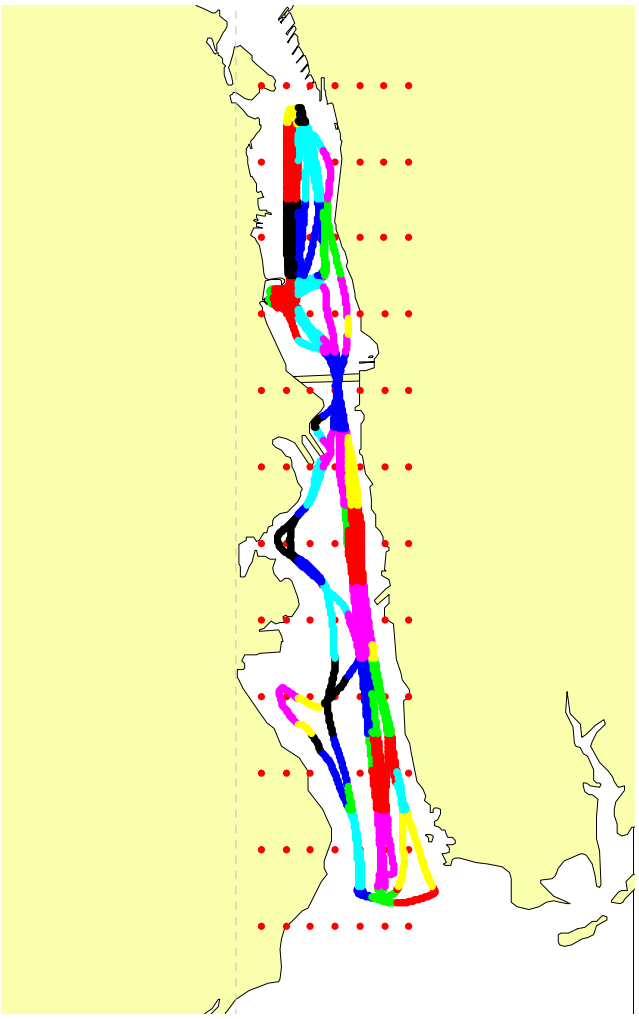

Figure 10 – Measured ASF grid for Thames River.

This disappointing performance called for further examination. Closer investigation shows that this uniform rectangular grid may not be the best approach. The data collection suffers from several problems: many of the grid points are on land and thus not measurable by boat, there are several points for which no data was collected, and most troublesome, the data was not collected uniformly at/around each grid point. These issues are shown in Figure 11 which is a close-up of Figure 10. The black points are collected somewhat uniformly around the grid point; however the green points are not. The median value for the green points is mapped to a grid point some distance away and not the center of the measured data, introducing an error into the grid, especially significant for areas with sharp change in ASF.

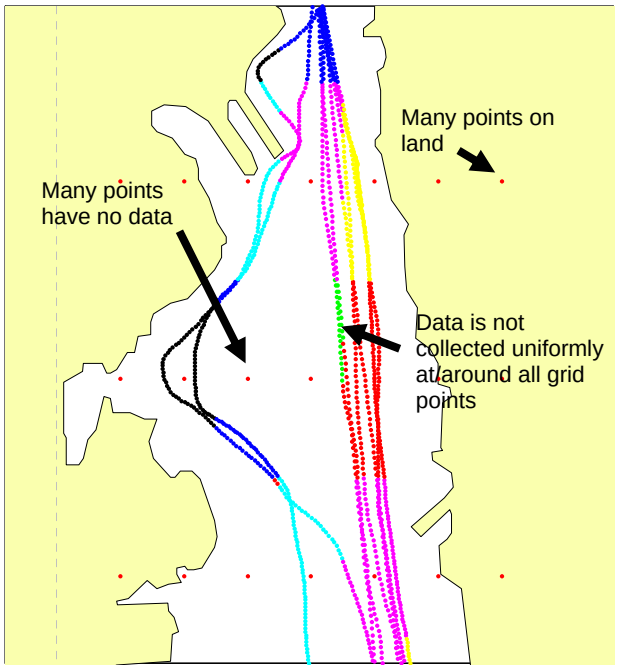

Figure 11 – close-up of Figure 10 illustrating some of the problems with the uniform grid.

The results of applying the ASF grids to Loran TOAs are shown in Figure 12. In this figure, the green crosses are the GPS positions which are used as ground truth. The magenta points are the raw Loran positions which exhibit the typical 600m error offset from truth. The dark blue points are the positions calculated using the Loran data corrected using the BALOR grid ASFs interpolated using bilinear interpolation. The light blue points are a similar grid interpolation using the real ASF grid where grid points with no data were filled with an average value. The black points are the same real data with the grid points without data eliminated; with a triangular interpolation of the three closest grid points used.

None of these grids gives great results due to the inaccuracies in the grids. If the actual ASF values were used the Loran+ASF track would be on top of the GPS track. In the future we will investigate using non-uniform grids. Some possibilities include using K-means clustering to clump data to a grid point at the center of the cluster vice having the grid point locations determined a priori based on an even rectangular grid. Other options are to grid only the areas of interest such as channels and navigable areas vice a rectangle over the entire area. This leads to vectors of Lat, Long and ASFs vice an even grid. There are interpolation techniques such as a triangular interpolation (surface fit) that can be used though. A 1 ns quantization on the ASF data is probably sufficient; however, sufficient data needs to be taken at each grid point such that the measurement noise is low (low standard deviation).

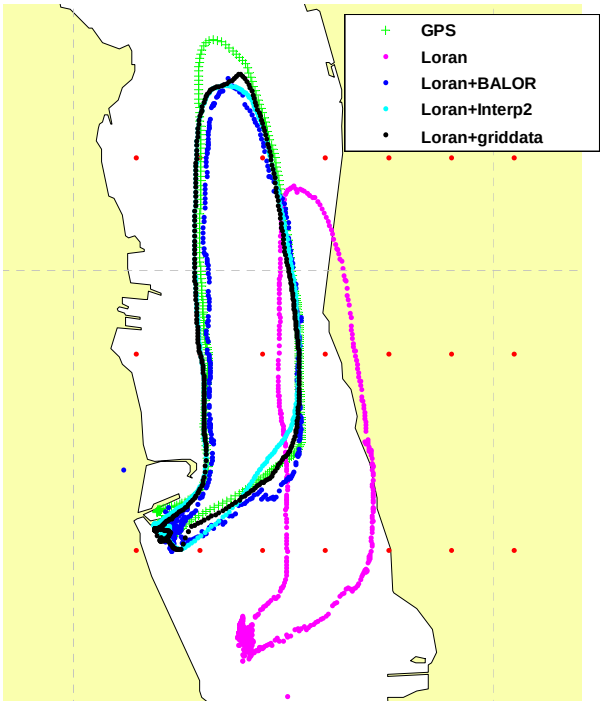

Figure 12 – ASF grid performance

INTEGRATED RECEIVER

Our motivation for using an integrated receiver is that an accurate position source is needed in the absence of GPS. The ASFs correct for the major source of error in a Loran position; however, 20m is a difficult accuracy target to attain. We need to account for Loran receiver errors as well and still meet the 20m target.

Our concept for an integrated Loran/GPS/IMU receiver is as follows. We do not integrate the Loran TOAs with GPS pseudoranges as the Loran receiver really does nothing to improve the GPS position solution. The intention is to have a receiver that can continue to provide accurate positions (Loran only) in the absence of GPS. The GPS receiver is used to track the ASF values in real-time in order to calculate the temporal correction to the ASF spatial grid. This temporal correction is updated as long as GPS is present. When GPS is lost, this temporal correction is then used to correct the spatial grid when the spatial grid is used in the Loran position solution. The IMU provides heading and velocity information that is integrated with the Loran TOA measurements in order to smooth out the TOA measurements and prevent position jumps due to receiver errors.

INERTIAL MEASURING UNIT (IMU)

The IMU we have chosen to use is a MEMs-based unit from Crossbow, Inc. (Figure 13). This unit, like other units based on MEMs technology, is low-cost but has poor long-term stability. This unit provides accelerations

in the x, y, and z directions as well as the angular accelerations around each axis (roll, pitch, and yaw) shown in Figure 14. These can be integrated to provide velocities and changes in unit attitude. The typical performance of this unit is shown in Figures 15 and 16 which show data collected on the Thames River. The blue lines are the raw acceleration data that has been un-biased. The red lines are the filtered data. Due to the noise present in the data, filtering is necessary.

Figure 13 – Crossbow IMU

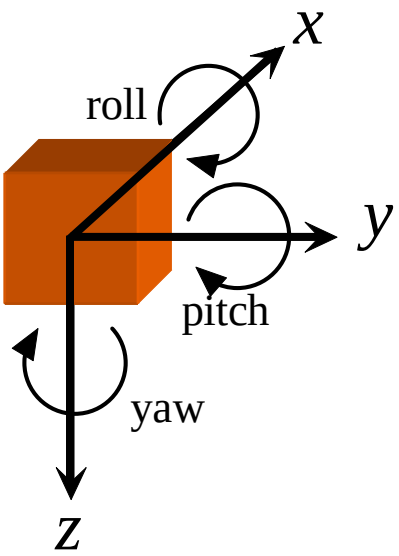

Figure 14 – IMU axis orientation

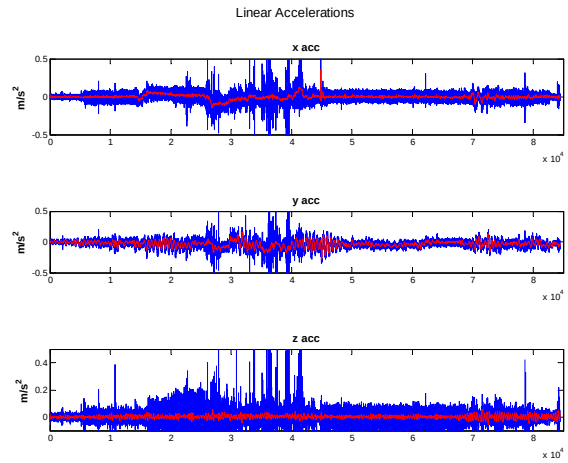

Figure 15 – IMU Linear acceleration data

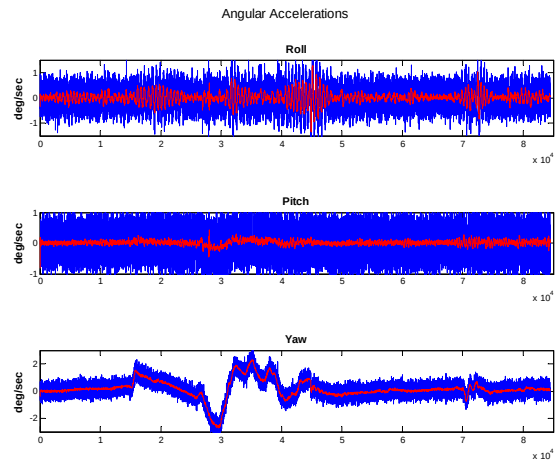

Figure 16 – Angular acceleration data

KALMAN FILTER

To integrate the IMU with the Loran data we have implemented an extended Kalman filter. In the extended Kalman filter, the IMU is used to create the reference trajectory. The IMU data is used to predict forward to the next position. This predicted position is used to calculate the TOAs and is also used to interpolate in the ASF grid to get the ASF values. The difference between these predicted TOAs and the measured TOAs (corrected by the ASF value) is taken. The difference is checked for possible cycle slips, and corrected if necessary, and then this TOA error (difference between predicted and measured) is used as the input to the Kalman filter. The output of the Kalman filter is the position error which is used to correct the predicted position.

The Kalman filter states are the standard states for integrating an IMU:

- X1 = east position error
- X2 = east velocity error
- X3 = tilt about y axis
- X4 = north position error
- X5 = north velocity error
- X6 = tilt about x axis
- X7 = vertical position error
- X8 = vertical velocity error
- X9 = azimuth error

Classical Kalman filtering begins with an estimate of the state $\hat{x}(0|0)$ and its covariance matrix $P(0|0)$. Given N observations, the actual filtering is the iteration over k, $k = 1, 2, \ldots N$, of three steps:

Project the state vector and its covariance matrix ahead one time step

$$\hat{x}(k|k-1) = \phi_k \; \hat{x}(k-1|k-1)$$

$$P(k|k-1) = \phi_k \; P(k-1|k-1) \; \phi_k^{\;T} + Q_k$$

Compute the Kalman filter gain

$$K_k = P(k|k-1) \; H^T \left(H \; P(k-1|k-1) \; H^T + R_k \right)^{-1}$$

Update the estimate and its covariance using an observation

$$\hat{x}(k|k) = \hat{x}(k|k-1) + K_k \left(y_k - H \; \hat{x}(k|k-1) \right)$$

$$P(k|k) = \left(I - K_k \; H \right) P(k|k-1)$$

Figure 17 shows the results of using the Kalman filter on date from the Thames River. In this case the green crosses are the GPS track which are used as the ground truth and the red dots are the raw Loran positions showing the typical 600m error. The blue dots are the Loran positions computed using ASF values from the grid. The black dots are the positions computed by the Kalman filter. Most of the time the Kalman filter yields better results than the Loran+ASF alone, but not in all cases, and the Kalman results are not quite as good as we would like so there is still some work to be done.

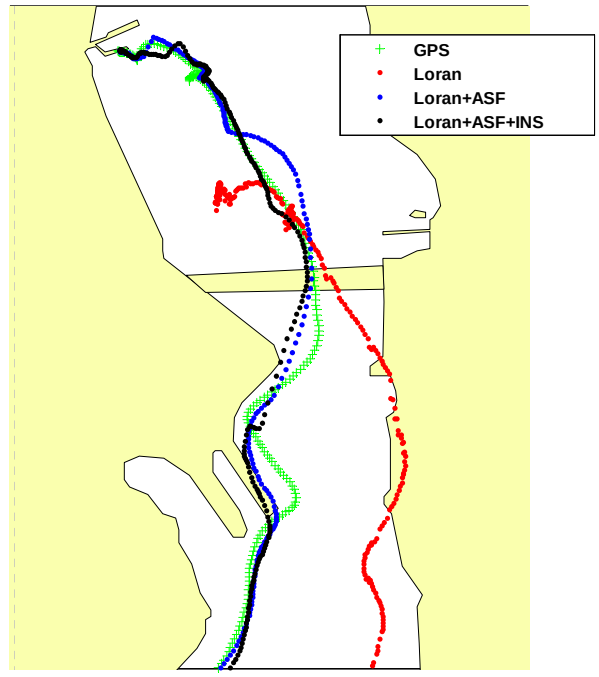

Figure 17 – Kalman filter performance

CONCLUSIONS / FUTURE

The Loran solution performance is very sensitive to the accuracy of the ASF grid. Based on the results to date, further work is needed on grid development for the maritime application. We will focus in the future on using a non-uniform vice a uniform grid and measuring the ASFs on the grid accurately. Further work is also needed on the IMU. We need a better estimate of the IMU bias so it can be removed. We also need to integrate the IMU into the system in real-time vice in a post-process mode.

The Kalman filter appears to work to smooth the position solutions; however it needs to be fine-tuned. We also need to extend it into a predictor to account for the Loran position lag due to the filtering (averaging of pulses) in the Loran receiver.

ACKNOWLEDGMENTS

The authors would like to thank the JJMA team that collected the data used in this analysis and Mr. Mitch Narins of the FAA who is the sponsor of this work.

REFERENCES

[1] Volpe National Transportation Systems Center, U.S. Department of Transportation, Office of Ass't Sec for Transportation Policy, "*Vulnerability Assessment of the Transportation Infrastructure Relying on the Global Positioning System*," Boston, MA, August 2001.

[2] Federal Aviation Administration, Office of Architecture and Investment Analysis, ASD-1, "*Navigation and Landing Transition Strategy*," Washington, DC, August 2002.

[3] R. Hartnett, G. Johnson, P. F. Swaszek, and M. J. Narins, "A Preliminary Study of LORAN-C Additional Secondary Factor (ASF) Variations," presented at 31st Annual Meeting, International Loran Association, Washington, DC, 28-30 October 2002.

[4] G. Johnson, R. Hartnett, et al., "FAA Loran-C Propagation Studies," presented at Annual Technical Meeting, Institute of Navigation, Anaheim, CA, 22-24 January 2003.

[5] G. Johnson, R. Hartnett, et al., "Summer Vacation 2003 - ASF Spatial Mapping in CO, AR, FL, and CA," presented at 32nd Annual Meeting, International Loran Association, Boulder, CO, 3-6 November 2003.

[6] P. Swaszek, G. Johnson, et al., "A Demonstration of High Accuracy Loran-C for Harbor Entrance and Approach Areas," presented at Fifty-ninth Annual Meeting, Institute of Navigation, Albuquerque, NM, 23-25 June 2003.

[7] R. Hartnett, G. Johnson, and P. Swaszek, "Navigating Using an ASF Grid For Harbor Entrance And Approach," presented at Institute of Navigation, Annual Meeting, Dayton, OH, 6 - 9 June 2004.

[8] G. Johnson, R. Shalaev, R. Hartnett, and P. Swaszek, "Can Loran Meet GPS backup Requirements?," presented at 11th Saint Petersburg International Conference on Integrated Navigation Systems, Saint Petersburg, RU, 24 - 26 May 2004.

[9] P. Williams and D. Last, "Modelling Loran-C Envelope-to-Cycle Differences in Mountainous Terrain," presented at 32nd Annual Meeting, International Loran Association, Boulder, CO, 3-6 November 2003.

[10] D. Last and P. Williams, "Loran-C ASF, Field Strength and ECD Modelling," presented at LORIPP meeting, Tysons Corner, VA, 29 July 2003.

[11] G. Johnson, C. Oates, et al., "Meeting Aviation Requirements for eLoran - An Improved H-field Antenna," presented at 33rd Annual Symposium of the International Loran Association, Tokyo, JA, 25 - 27 October 2004.

DISCLAIMER AND NOTE

The views expressed herein are those of the authors and are not to be construed as official or reflecting the views of the U.S. Coast Guard, Federal Aviation Administration, or any agency of the U.S. Government.